AIAA JOURNAL
Vol. 42, No. 5, May 2004

Electroelastic Analysis of Piezoelectric Composite Laminates by Boundary Integral Equations

Giuseppe Davì* and Alberto Milazzo†
Università di Palermo, 90128 Palermo, Italy

A boundary integral representation for the electroelastic state in piezoelectric composite laminates subjected to axial extension, bending, torsion, shear/bending, and electric loadings is proposed. The governing equations are presented in terms of electromechanical generalized variables by the use of a suitable matrix notation. Thus, the three-dimensional electroelasticity solution for piezoelectric composite laminates is generated from a set of two partially coupled differential equations defined on the cross section of each individual ply within the laminate. These ply equations are linked through the interface conditions, which allow restoration of the model of the laminate as a whole. For this model, the corresponding boundary integral representation and the relative boundary integral equations are deduced, and their features are discussed. The formulation presented lays out the analytical foundation for the development of the multidomain boundary element method to determine numerically the electromechanical response of piezoelectric composite laminates. Numerical results showing the characteristics of the method are given, and the fundamental behavior of piezoelectric composite laminates is pointed out for both mechanical and electrical loads.

I. Introduction

PIEZOELECTRIC materials generate an electric field when subjected to strain fields and undergo deformation when an electric field is applied. This inherent electromechanical coupling, known as direct and converse piezoelectric effects, is widely exploited in the design of many devices working as transducers, sensors, and actuators. In addition, piezoelectric materials are of primary concern in the field of advanced lightweight structures, where the smart structure technology is now emerging.[1–4]

When piezoelectric members are bonded or merged within a structure, it is possible to combine the mechanical properties of the host structure with the additional capabilities to sense deformation and to adapt the structural response accordingly. The first attempt at the application of smart structures with sensing and control capabilities was concerned with the application of piezoelectric patches on the surfaces of beams and plates to induce strain actions on the passive structure or detect its deformation. The development of this approach, together with the improvement of composite material technology, led to the concept of distributed sensing and control, which can be accomplished by the introduction of piezoelectric layers within composite laminates. More recently, the idea of distributed structural control properties has been fully developed by the use of active fiber composites.[5] In these fiber-reinforced composites, the fiber and the matrix have additional functions besides their typical roles. The fiber, which generally exhibits a piezoelectric behavior, not only accomplishes the task of structural reinforcement, but it also has the function of both sensor and actuator. In this kind of smart structure, an active control of the mechanical response is performed on the basis of the intrinsic properties of the structure material. Some of the fundamental problems involved in the mechanical testing, analysis, and design, namely, failure modes and strength and stiffness degradation under static and cyclic fatigue loads, are not tractable without a thorough knowledge of the three-dimensional state of stress and deformation and of the electric influence on these quantities, especially in the boundary-layer regions. Again, the identification of effective sensing and actuating capacities of piezoelectric composite laminates and, consequently, the design of efficient control laws, are strictly related to the determination of the electromechanical state.

The preceding considerations make it imperative to establish complete and accurate solutions for piezoelectric laminates loaded by both mechanical and electric loads. Many theories and models have been proposed for the analysis of laminated composites with active and passive piezoelectric patches or layers. Some of these theories are based on simplifying assumptions to model the induced strain or electric field generated by piezoelectric layers (as in Refs. 6–8). Exact solutions for the problem have been given by authors who employed the separate-variable method for piezoelectric laminates both in cases of cylindrical bending[9] and simply supported laminates,[10,11] the Eshelby–Stroh formalism for laminates in cylindrical bending[12] and the transfer matrix approach for simply supported laminates.[13,14] Closed-form analytical solutions are also available for one-dimensional beams.[15] These solutions show the crucial role played by an accurate appraisal of the electromechanical response and the need for careful numerical simulations for complex configurations. Some finite element solutions for piezoelectric solids were proposed,[16–18] and the finite element method was successfully applied to general piezoelectric problems, as shown by the extensive literature on the subject.[19] In particular, finite elements for laminated composites with piezoelectric layers have been developed based on coupled layerwise theories.[20–26] Notwithstanding, many of the available finite element formulations for beams and plates do not account for the full electromechanical coupling, evidencing a lack in the capability to analyze specific topics. More recently, the boundary element method (BEM) has been used to solve both two-dimensional[27–30] and three-dimensional[31,32] piezoelectric problems. It was proved accurate and very efficient, particularly when the investigation concerns two-dimensional piezoelastic bodies for which the fundamental solutions are known in closed form.[27–30]

In the present paper, a boundary integral model for the analysis of piezoelectric composite laminates is presented. The formulation is based on an approach previously proposed by the authors for the analysis of classical composite laminates[33–37] that proved to be an interesting and effective tool for composite laminate structural analysis and that was partially extended to piezoelectric laminates in previous works.[38–40] In the approach, piezoelectric laminates subjected to axial, bending, torsion, shear/bending, and electric loadings are

Received 7 May 2002; revision received 23 October 2003; accepted for publication 3 December 2003.

*Full Professor, Dipartimento di Ingegneria Aeronautica e dei Transporti, Viale delle Scienze; davi@unipa.it. Member AIAA.
†Associate Professor, Dipartimento di Ingegneria Aeronautica e dei Transporti, Viale delle Scienze; milazzo@diat.unipa.it. Member AIAA.

dealt with by the introduction of the electromechanical generalized variables. This leads to the generation of a system of two partially coupled partial differential equations that govern the electromechanical response of each ply within the laminate in terms of generalized displacement functions defined on the ply cross section. The corresponding boundary integral equations are obtained starting from the reciprocity theorem and by the use of the analytic fundamental solutions of two-dimensional piezoelasticity. Then the piezoelectric laminate model is recovered by the imposition of the appropriate interface continuity and boundary conditions. This gives the basis for the development of the numerical solution by the multidomain BEM, whose implementation is discussed. Finally, the convergence characteristics, accuracy, aptitude, and effectiveness of the approach are ascertained with the aim to address the fundamental topics of the formulation and the basic characteristics of piezoelectric laminate behavior from both mechanical and electric points of view.

II. Governing Equations for Piezoelectric Laminates

Let us consider a beam-type piezoelectric composite laminate referred to the coordinate system $x_1x_2x_3$ with the $x_3 \equiv z$ axis parallel to the generators of the lateral surface, as shown in Fig. 1. The laminate consists of N piezoelectric anisotropic prismatic plies with a general layup. Each individual ply has a cross section $\Omega_{\langle k\rangle}$ with boundary $\partial\Omega_{\langle k\rangle}$, where the subscript $\langle k\rangle$ denotes quantities related to the kth ply. The plies are perfectly bonded along the interfaces $\partial\Omega_{mn}$ where the notation indicates the interface between the mth and nth plies. The laminate is subjected to load actions applied at its ends, resulting in axial extension, bending, twisting, and shear/bending. It is also subjected to electrical loads in the form of electric potential applied at its free surfaces and/or interfaces. According to Barnett and Lothe,[41] the piezoelectric problem can be described by the introduction of suitable electroelastic quantities, namely, the electromechanical generalized variables. These are the generalized displacements $\boldsymbol{S} = [s_1 \;\; s_2 \;\; s_3 \;\; \varphi]^T$ whose components are the displacements s_i and the electric potential φ; the generalized strains $\boldsymbol{\Gamma} = [\gamma_{11} \;\; \gamma_{22} \;\; \gamma_{33} \;\; \gamma_{32} \;\; \gamma_{31} \;\; \gamma_{21} \;\; -E_1 \;\; -E_2 \;\; -E_3]^T$ defined by collection of the strains γ_{ij} and the opposite of the electric field components E_i; the generalized stresses $\Sigma = [\sigma_{11} \;\; \sigma_{22} \;\; \sigma_{33} \;\; \sigma_{32} \;\; \sigma_{31} \;\; \sigma_{21} \;\; D_1 \;\; D_2 \;\; D_3]^T$ obtained by collection of the stresses σ_{ij} and the electric displacements D_i; the generalized body forces $\boldsymbol{F} = [f_1 \;\; f_2 \;\; f_3 \;\; -q]^T$ having components given by the body forces f_i and the opposite of the electric charge density q; and the generalized tractions $\boldsymbol{T}$ and/or $\boldsymbol{\Psi}$ given by the mechanical tractions and the normal component of the electric displacement.

By virtue of Saint Venant's principle, sufficiently far from the laminate ends, the generalized displacement field $\boldsymbol{S}$ can be expressed as[42,43]

$$\boldsymbol{S} = \boldsymbol{U} + z\boldsymbol{V} + \left[z\boldsymbol{X}_1 + \tfrac{1}{2}z^2(\boldsymbol{X}_2 - \boldsymbol{X}_3) - \tfrac{1}{6}z^3\boldsymbol{X}_4\right]\boldsymbol{k} \tag{1}$$

where the rigid motion terms have been dropped and $\boldsymbol{U} = [u_1 \;\; u_2 \;\; u_3 \;\; \varphi_0]^T$ and $\boldsymbol{V} = [v_1 \;\; v_2 \;\; v_3 \;\; \varphi_l]^T$ are vectors of generalized displacement functions depending on x_1 and x_2 only. The matrices $\boldsymbol{X}_i$ are defined as

$$\boldsymbol{X}_1 = \begin{bmatrix} 0 & 0 & 0 & -x_2 & 0 & 0 \\ 0 & 0 & 0 & x_1 & 0 & 0 \\ 1 & x_1 & x_2 & 0 & 0 & 0 \\ 0 & 0 & 0 & 0 & 0 & 0 \end{bmatrix} \tag{2}$$

$$\boldsymbol{X}_2 = \begin{bmatrix} 0 & 0 & 0 & 0 & 0 & 0 \\ 0 & 0 & 0 & 0 & 0 & 0 \\ 0 & 0 & 0 & 0 & x_1 & x_2 \\ 0 & 0 & 0 & 0 & 0 & 0 \end{bmatrix} \tag{3}$$

$$\boldsymbol{X}_3 = \begin{bmatrix} 0 & 1 & 0 & 0 & 0 & 0 \\ 0 & 0 & 1 & 0 & 0 & 0 \\ 0 & 0 & 0 & 0 & 0 & 0 \\ 0 & 0 & 0 & 0 & 0 & 0 \end{bmatrix} \tag{4}$$

$$\boldsymbol{X}_4 = \begin{bmatrix} 0 & 0 & 0 & 0 & 1 & 0 \\ 0 & 0 & 0 & 0 & 0 & 1 \\ 0 & 0 & 0 & 0 & 0 & 0 \\ 0 & 0 & 0 & 0 & 0 & 0 \end{bmatrix} \tag{5}$$

In Eq. (1), $\boldsymbol{k} = [\varepsilon_0 \;\; \kappa_1 \;\; \kappa_2 \;\; \vartheta \;\; \gamma_1 \;\; \gamma_2]^T$ is the mechanical loading vector whose components are the laminate axial extension, the two bending curvatures, the twisting, and the two bending curvatures for unit length associated with the shear/bending behavior. The derivation of the governing equations[41,44] for the electromechanical behavior of each single ply within the laminate is based on the idea of splitting the generalized equilibrium operator $\mathcal{D}$, so that the variations along the span are manifest. One has

$$\mathcal{D} = \mathcal{D}_x + \mathcal{D}_z = \mathcal{D}_x + \boldsymbol{I}_z\frac{\partial}{\partial z} =$$

$$\begin{bmatrix} \frac{\partial}{\partial x_1} & 0 & 0 & 0 \\ 0 & \frac{\partial}{\partial x_2} & 0 & 0 \\ 0 & 0 & 0 & 0 \\ 0 & 0 & \frac{\partial}{\partial x_2} & 0 \\ 0 & 0 & \frac{\partial}{\partial x_1} & 0 \\ \frac{\partial}{\partial x_2} & \frac{\partial}{\partial x_1} & 0 & 0 \\ 0 & 0 & 0 & \frac{\partial}{\partial x_1} \\ 0 & 0 & 0 & \frac{\partial}{\partial x_2} \\ 0 & 0 & 0 & 0 \end{bmatrix} + \begin{bmatrix} 0 & 0 & 0 & 0 \\ 0 & 0 & 0 & 0 \\ 0 & 0 & 1 & 0 \\ 0 & 1 & 0 & 0 \\ 1 & 0 & 0 & 0 \\ 0 & 0 & 0 & 0 \\ 0 & 0 & 0 & 0 \\ 0 & 0 & 0 & 0 \\ 0 & 0 & 0 & 1 \end{bmatrix} \frac{\partial}{\partial z} \tag{6}$$

so that the generalized strains are given by

$$\boldsymbol{\Gamma} = \mathcal{D}_x\boldsymbol{U} + \boldsymbol{I}_z\boldsymbol{V} + \boldsymbol{I}_z\boldsymbol{X}_1\boldsymbol{k} + z(\mathcal{D}_x\boldsymbol{V} + \boldsymbol{I}_z\boldsymbol{X}_2\boldsymbol{k}) = \boldsymbol{\Gamma}_U + z\boldsymbol{\Gamma}_V \tag{7}$$

Introducing the ply generalized stiffness matrix $\boldsymbol{R}_{\langle k\rangle}$ (Ref. 45) from the constitutive equations, one obtains the generalized stresses of the kth ply, which are given by

$$\Sigma = \boldsymbol{R}_{\langle k\rangle}\mathcal{D}_x\boldsymbol{U} + \boldsymbol{R}_{\langle k\rangle}\boldsymbol{I}_z\boldsymbol{V} + \boldsymbol{R}_{\langle k\rangle}\boldsymbol{I}_z\boldsymbol{X}_1\boldsymbol{k} + z\left(\boldsymbol{R}_{\langle k\rangle}\mathcal{D}_x\boldsymbol{V} + \boldsymbol{R}_{\langle k\rangle}\boldsymbol{I}_z\boldsymbol{X}_2\boldsymbol{k}\right) = \Sigma_U + z\Sigma_V \tag{8}$$

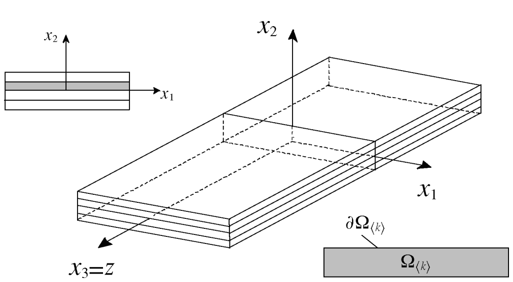

Fig. 1 Typical laminate configuration and reference system.

Then the generalized equilibrium equations of the kth ply can be written in terms of generalized displacement functions as

$$\mathcal{D}^T\Sigma = \mathcal{D}_x^T \boldsymbol{R}_{\langle k\rangle}\mathcal{D}_x\boldsymbol{U} + \left(\mathcal{D}_x^T\boldsymbol{R}_{\langle k\rangle}\boldsymbol{I}_z + \boldsymbol{I}_z^T\boldsymbol{R}_{\langle k\rangle}\mathcal{D}_x\right)\boldsymbol{V} + \mathcal{D}_x^T\boldsymbol{R}_{\langle k\rangle}\boldsymbol{I}_z\boldsymbol{X}_1\boldsymbol{k} + \boldsymbol{I}_z^T\boldsymbol{R}_{\langle k\rangle}\boldsymbol{I}_z\boldsymbol{X}_2\boldsymbol{k} + z\left(\mathcal{D}_x^T\boldsymbol{R}_{\langle k\rangle}\mathcal{D}_x\boldsymbol{V} + \mathcal{D}_x^T\boldsymbol{R}_{\langle k\rangle}\boldsymbol{I}_z\boldsymbol{X}_2\boldsymbol{k}\right) = \boldsymbol{0} \tag{9}$$

The generalized tractions on the kth ply lateral surface are given by

$$\boldsymbol{T} = \mathcal{D}_{xn}^T\boldsymbol{R}_{\langle k\rangle}\mathcal{D}_x\boldsymbol{U} + \mathcal{D}_{xn}^T\boldsymbol{R}_{\langle k\rangle}\boldsymbol{I}_z\boldsymbol{V} + \mathcal{D}_{xn}^T\boldsymbol{R}_{\langle k\rangle}\boldsymbol{I}_z\boldsymbol{X}_1\boldsymbol{k} + z\left(\mathcal{D}_{xn}^T\boldsymbol{R}_{\langle k\rangle}\mathcal{D}_x\boldsymbol{V} + \mathcal{D}_{xn}^T\boldsymbol{R}_{\langle k\rangle}\boldsymbol{I}_z\boldsymbol{X}_2\boldsymbol{k}\right) = \boldsymbol{T}_U + z\boldsymbol{T}_V \tag{10}$$

where $\mathcal{D}_{xn}$ is the generalized boundary traction operator obtained from the differential operator $\mathcal{D}$ by replacement of the derivatives with the corresponding direction cosines of the outer normal to the boundary of the ply cross section. Likewise, the generalized tractions on the cross section of the kth ply are given by

$$\boldsymbol{\Psi} = \boldsymbol{I}_z^T\boldsymbol{R}_{\langle k\rangle}\mathcal{D}_x\boldsymbol{U} + \boldsymbol{I}_z^T\boldsymbol{R}_{\langle k\rangle}\boldsymbol{I}_z\boldsymbol{V} + \boldsymbol{I}_z^T\boldsymbol{R}_{\langle k\rangle}\boldsymbol{I}_z\boldsymbol{X}_1\boldsymbol{k} + z\left(\boldsymbol{I}_z^T\boldsymbol{R}_{\langle k\rangle}\mathcal{D}_x\boldsymbol{V} + \boldsymbol{I}_z^T\boldsymbol{R}_{\langle k\rangle}\boldsymbol{I}_z\boldsymbol{X}_2\boldsymbol{k}\right) = \boldsymbol{\Psi}_U + z\boldsymbol{\Psi}_V \tag{11}$$

Note that $\boldsymbol{I}_z$ is the generalized cross section traction operator obtained from $\mathcal{D}$ by replacement of the derivatives with the corresponding direction cosines of the outer normal to the ply cross section. Equation (9) is verified to fulfill the following expressions simultaneously:

$$\mathcal{D}_x^T\boldsymbol{R}_{\langle k\rangle}\mathcal{D}_x\boldsymbol{V} + \mathcal{D}_x^T\boldsymbol{R}_{\langle k\rangle}\boldsymbol{I}_z\boldsymbol{X}_2\boldsymbol{k} = \boldsymbol{0} \tag{12}$$

$$\mathcal{D}_x^T\boldsymbol{R}_{\langle k\rangle}\mathcal{D}_x\boldsymbol{U} + \left(\mathcal{D}_x^T\boldsymbol{R}_{\langle k\rangle}\boldsymbol{I}_z + \boldsymbol{I}_z^T\boldsymbol{R}_{\langle k\rangle}\mathcal{D}_x\right)\boldsymbol{V} + \mathcal{D}_x^T\boldsymbol{R}_{\langle k\rangle}\boldsymbol{I}_z\boldsymbol{X}_1\boldsymbol{k} + \boldsymbol{I}_z^T\boldsymbol{R}_{\langle k\rangle}\boldsymbol{I}_z\boldsymbol{X}_2\boldsymbol{k} = \boldsymbol{0} \tag{13}$$

These equations constitute a partially coupled system of partial differential equations defined on the ply cross section. The preceding set of equations, together with the boundary conditions expressed in terms of $\boldsymbol{V}$ and $\boldsymbol{T}_V$ for Eq. (12) and $\boldsymbol{U}$ and $\boldsymbol{T}_U$ for Eq. (13), governs the electromechanical behavior of each individual ply within the laminate. The model for the piezoelectric laminate as a whole is obtained when the individual ply governing equations are linked through the interface generalized continuity conditions along the interfaces. If the interface $\partial\Omega_{mn}$ is only a bonding surface, these conditions state that, along the interface, the generalized displacement functions $\boldsymbol{U}$ and $\boldsymbol{V}$ of the mth and nth ply have to be equal, whereas the corresponding generalized traction functions $\boldsymbol{T}_V$ and $\boldsymbol{T}_U$ have to be opposite. On the other hand, if the interface $\partial\Omega_{mn}$ is an electroded interface, then the electric potential on this surface is a known function and the normal component of the electric displacement does not need to be continuous across the interface. Thus, the interface conditions on $\partial\Omega_{mn}$ are given in terms of prescribed electric potential functions φ_0 and φ_l, equality of the displacement functions u_i and v_i of the mth and nth ply, and equilibrium of the corresponding mechanical traction functions along the interface.[12] Finally, the laminate response is defined by the relationship between the loading vector $\boldsymbol{k}$ and the corresponding mechanical load vector $\boldsymbol{P} = [N\ \ M_1\ \ M_2\ \ M_t\ \ V_1\ \ V_2]^T$, whose components are the axial force, bending and twisting moments, and shear forces. These are given by the laminate cross section equilibrium conditions, which, at a given span station $\bar{z}$, read as

$$\sum_1^N \int_{\Omega_{\langle k\rangle}} (\boldsymbol{X}_1 + \boldsymbol{X}_4)^T\boldsymbol{I}_z^T\boldsymbol{R}_{\langle k\rangle}(\mathcal{D}_x\boldsymbol{U} + \boldsymbol{I}_z\boldsymbol{V} + \bar{z}\mathcal{D}_x\boldsymbol{V})\,\mathrm{d}\Omega + \left[\sum_1^N \int_{\Omega_{\langle k\rangle}} (\boldsymbol{X}_1 + \boldsymbol{X}_4)^T\boldsymbol{I}_z^T\boldsymbol{R}_{\langle k\rangle}\boldsymbol{I}_z(\boldsymbol{X}_1 + \bar{z}\boldsymbol{X}_2)\,\mathrm{d}\Omega\right]\boldsymbol{k} = \boldsymbol{P} \tag{14}$$

III. Reciprocity Statement for Piezoelectric Ply

Let $\boldsymbol{S}_j$ be a particular system of generalized displacements associated with a system of generalized body forces denoted by $\boldsymbol{F}_j$, so that

$$\mathcal{D}^T\boldsymbol{R}\mathcal{D}\boldsymbol{S}_j + \boldsymbol{F}_j = \boldsymbol{0} \tag{15}$$

Let $\boldsymbol{\Gamma}_j$, Σ_j, and $\boldsymbol{T}_j$ and $\boldsymbol{\Psi}_j$ be the generalized strain, stress, and traction fields due to $\boldsymbol{S}_j$, respectively. When the generalized variables notation and the symmetry of the generalized stiffness matrix are resorted to, the following reciprocity theorem for piezoelasticity is written[29,45]

$$\int_{\partial\mathcal{V}} \left(\boldsymbol{T}_j^T\boldsymbol{S} - \boldsymbol{S}_j^T\boldsymbol{T}\right)\mathrm{d}\partial\mathcal{V} + \int_{\mathcal{V}} \left(\boldsymbol{F}_j^T\boldsymbol{S} - \boldsymbol{S}_j^T\boldsymbol{F}\right)\mathrm{d}\mathcal{V} = 0 \tag{16}$$

where $\mathcal{V}$ is the volume occupied by the piezoelectric body and $\partial\mathcal{V}$ is the corresponding boundary. To apply the reciprocity theorem to the generic ply within the laminate, consider an elementary slice of this prismatic ply included between two cross sections with an infinitesimal distance $\mathrm{d}z$. The elementary slice occupies the volume $\mathcal{V} \equiv \Omega_{\langle k\rangle}\cdot \mathrm{d}z$, which is bounded by the two cross sections $\Omega_{\langle k\rangle}$ and by the lateral surface $\partial\mathcal{V} \equiv \partial\Omega_{\langle k\rangle}\cdot\mathrm{d}z$. Equation (16) is then written as follows:

$$\int_{\partial\Omega_{\langle k\rangle}} \left(\boldsymbol{T}_j^T\boldsymbol{S} - \boldsymbol{S}_j^T\boldsymbol{T}\right)\mathrm{d}\partial\Omega\,\mathrm{d}z + \int_{\Omega_{\langle k\rangle}} \left[\left(\boldsymbol{\Psi}_j^T\boldsymbol{S} - \boldsymbol{S}_j^T\boldsymbol{\Psi}\right) + \frac{\partial}{\partial z}\left(\boldsymbol{\Psi}_j^T\boldsymbol{S} - \boldsymbol{S}_j^T\boldsymbol{\Psi}\right)\mathrm{d}z\right]\mathrm{d}\Omega - \int_{\Omega_{\langle k\rangle}} \left(\boldsymbol{\Psi}_j^T\boldsymbol{S} - \boldsymbol{S}_j^T\boldsymbol{\Psi}\right)\mathrm{d}\Omega + \int_{\Omega_{\langle k\rangle}} \left(\boldsymbol{F}_j^T\boldsymbol{S} - \boldsymbol{S}_j^T\boldsymbol{F}\right)\mathrm{d}\Omega\,\mathrm{d}z = 0 \tag{17}$$

and, when $\mathrm{d}z$ approaches zero, one obtains

$$\int_{\partial\Omega_{\langle k\rangle}} \left(\boldsymbol{T}_j^T\boldsymbol{S} - \boldsymbol{S}_j^T\boldsymbol{T}\right)\mathrm{d}\partial\Omega + \int_{\Omega_{\langle k\rangle}} \frac{\partial}{\partial z}\left(\boldsymbol{\Psi}_j^T\boldsymbol{S} - \boldsymbol{S}_j^T\boldsymbol{\Psi}\right)\mathrm{d}\Omega + \int_{\Omega_{\langle k\rangle}} \left(\boldsymbol{F}_j^T\boldsymbol{S} - \boldsymbol{S}_j^T\boldsymbol{F}\right)\mathrm{d}\Omega = 0 \tag{18}$$

Equation (18) is the expression of the piezoelectricity generalized reciprocity theorem inherent to the laminate analysis problem. It is the starting point from which to derive the boundary integral representation of the generalized displacements field.

IV. Generalized Displacements Boundary Integral Representation

Let us assume that the generalized displacements $\boldsymbol{S}_j$ are associated with a system of generalized body forces constant along the z axis, namely, $\boldsymbol{F}_j = \boldsymbol{F}_j(x_1, x_2)$. This particular solution $\boldsymbol{S}_j$ is independent on the z coordinate. According to Eq. (1), one then has $\boldsymbol{S}_j = \boldsymbol{U}_j(x_1, x_2)$. Applying the reciprocity theorem for piezoelectric beam-type structures, that is, Eq. (18), to the particular solution introduced earlier and the actual elastic response of the ply within the laminate, one obtains

$$\int_{\partial\Omega_{\langle k\rangle}} \left(\boldsymbol{T}_j^T\boldsymbol{S} - \boldsymbol{U}_j^T\boldsymbol{T}\right)\mathrm{d}\partial\Omega + \int_{\Omega_{\langle k\rangle}} \boldsymbol{F}_j^T\boldsymbol{S}\,\mathrm{d}\Omega + \int_{\Omega_{\langle k\rangle}} \frac{\partial}{\partial z}\left(\boldsymbol{\Psi}_j^T\boldsymbol{S} - \boldsymbol{U}_j^T\boldsymbol{\Psi}\right)\mathrm{d}\Omega = 0 \tag{19}$$

On substitution for $\boldsymbol{S}$, $\boldsymbol{T}$, and $\boldsymbol{\Psi}$ from Eqs. (1), (10), and (11), respectively, Eq. (19) leads to a third-order polynomial expression in the z coordinate. By using the divergence theorem, one notes that, to verify this polynomial expression for every choice of z, the following set of equations has to be fulfilled simultaneously:

$$\int_{\partial\Omega_{\langle k\rangle}} \left(\boldsymbol{T}_j^T\boldsymbol{V} - \boldsymbol{U}_j^T\boldsymbol{T}_V\right)\mathrm{d}\partial\Omega + \int_{\Omega_{\langle k\rangle}} \boldsymbol{F}_j^T\boldsymbol{V}\,\mathrm{d}\Omega + \int_{\Omega_{\langle k\rangle}} \boldsymbol{\Psi}_j^T\boldsymbol{X}_2\boldsymbol{k}\,\mathrm{d}\Omega = 0 \tag{20}$$

$$\int_{\partial\Omega_{\langle k\rangle}} \left(\boldsymbol{T}_j^T\boldsymbol{U} - \boldsymbol{U}_j^T\boldsymbol{T}_U\right)\mathrm{d}\partial\Omega + \int_{\Omega_{\langle k\rangle}} \boldsymbol{F}_j^T\boldsymbol{U}\,\mathrm{d}\Omega + \int_{\Omega_{\langle k\rangle}} \left(\boldsymbol{\Psi}_j^T\boldsymbol{V} - \boldsymbol{U}_j^T\boldsymbol{\Psi}_V\right)\mathrm{d}\Omega + \int_{\Omega_{\langle k\rangle}} \boldsymbol{\Psi}_j^T\boldsymbol{X}_1\boldsymbol{k}\,\mathrm{d}\Omega = 0 \tag{21}$$

Hence, the piezoelasticity reciprocity theorem for the ply within the laminate reduces to the two integral relations (20) and (21), which are the basis from which to derive directly the integral representation employed in the method proposed. Actually, assume the generalized body forces $\boldsymbol{F}_j$ to be given by a line force load applied along a line parallel to the longitudinal axis z and a bulk charge density concentrated along the same line. By indication with P_0 and P the generalized load application point and the generic field point in the ply cross section, the representation of $\boldsymbol{F}_j$ is given by

$$\boldsymbol{F}_j = \boldsymbol{C}_j \delta(P - P_0) \tag{22}$$

where δ denotes the Dirac function and $\boldsymbol{C}_j$ is the representative vector of the generalized load. The generalized displacements field $\boldsymbol{U}_j = \boldsymbol{U}_j(P, P_0)$ and the corresponding generalized tractions $\boldsymbol{T}_j = \boldsymbol{T}_j(P, P_0)$ associated with this generalized load are the kernels of the singular fundamental solution of the problem. This fundamental solution is the electroelastic generalized plain strain ($\gamma_{33} = D_3 = 0$) response of the infinite two-dimensional piezoelectric domain loaded by concentrated generalized body forces applied at the point P_0. Its explicit, closed-form expression is given in Ref. 45. On application of Dirac function properties and of the divergence theorem, Eqs. (20) and (21) become

$$\boldsymbol{C}_j^T \boldsymbol{V}(P_0) = \int_{\partial\Omega_{\langle k\rangle}} \left(\boldsymbol{U}_j^T \boldsymbol{T}_V - \boldsymbol{T}_j^T \boldsymbol{V}\right) \mathrm{d}\partial\Omega - \int_{\Omega_{\langle k\rangle}} (\mathcal{D}_x \boldsymbol{U}_j)^T \boldsymbol{R}\boldsymbol{I}_z \boldsymbol{X}_2 \boldsymbol{k}\, \mathrm{d}\Omega \tag{23}$$

$$\begin{aligned}\boldsymbol{C}_j^T \boldsymbol{U}(P_0) = {}& \int_{\partial\Omega_{\langle k\rangle}} \left(\boldsymbol{U}_j^T \boldsymbol{T}_U - \boldsymbol{T}_j^T \boldsymbol{U}\right) \mathrm{d}\partial\Omega \\ & + \int_{\Omega_{\langle k\rangle}} \boldsymbol{U}_j^T \left(\mathcal{D}_x^T \boldsymbol{R}\boldsymbol{I}_z + \boldsymbol{I}_z^T \boldsymbol{R}\mathcal{D}_x\right) \boldsymbol{V}\, \mathrm{d}\Omega - \int_{\partial\Omega_{\langle k\rangle}} \boldsymbol{U}_j^T \mathcal{D}_{xn}^T \boldsymbol{R}\boldsymbol{I}_z \boldsymbol{V}\, \mathrm{d}\Omega \\ & - \int_{\Omega_{\langle k\rangle}} (\mathcal{D}_x \boldsymbol{U}_j)^T \boldsymbol{R}\boldsymbol{I}_z \boldsymbol{X}_1 \boldsymbol{k}\, \mathrm{d}\Omega + \int_{\Omega_{\langle k\rangle}} \boldsymbol{U}_j^T \boldsymbol{I}_z^T \boldsymbol{R}\boldsymbol{I}_z \boldsymbol{X}_2 \boldsymbol{k}\, \mathrm{d}\Omega \end{aligned} \tag{24}$$

Equations (23) and (24) are the form of the beam-type structure Somigliana identity in piezoelasticity, which consists of a set of two partially coupled integral relations. They provide a direct link between the generalized displacements functions $\boldsymbol{V}$ and $\boldsymbol{U}$ at the field point P_0 and the characteristics of the piezoelastic response on the boundary of the ply cross section, namely, the generalized displacements and the generalized tractions. By virtue of the partially coupled nature of these integral relations, the generalized displacement function $\boldsymbol{V}$ is expressed through Eq. (23) in terms of its boundary values and the corresponding generalized traction function $\boldsymbol{T}_V$. Once the generalized displacement function $\boldsymbol{V}$ is determined, Eq. (24) identifies the generalized displacement function $\boldsymbol{U}$ in terms of the relative boundary values and generalized traction function $\boldsymbol{T}_U$. All of the domain integrals appearing in Eqs. (23) and (24) actually involve known functions or quantities expressible in terms of boundary characteristics. Therefore, Eqs. (23) and (24) give a boundary integral representation of the generalized displacement field of the ply within the laminate. In addition, some of these domain integrals can be transformed into boundary integrals according to the particular solution technique.[35,36] To obtain this goal, consider a particular generalized displacement field $\bar{\boldsymbol{S}}$ that satisfies the ply governing field equations through suitable generalized displacement functions $\bar{\boldsymbol{U}}$ and $\bar{\boldsymbol{V}}$, for example, second-order polynomials of x_1 and x_2 (see Appendix). Writing the generalized displacements boundary integral representation for $\bar{\boldsymbol{S}}$ and combining it with Eqs. (23) and (24), one attains the following alternative form of the beam-type structure Somigliana identity for piezoelasticity:

$$\begin{aligned}\boldsymbol{C}_j^T \boldsymbol{V}(P_0) = {}& \int_{\partial\Omega_{\langle k\rangle}} \left(\boldsymbol{U}_j^T \boldsymbol{T}_V - \boldsymbol{T}_j^T \boldsymbol{V}\right) \mathrm{d}\partial\Omega \\ & + \int_{\partial\Omega_{\langle k\rangle}} \left(\boldsymbol{T}_j^T \bar{\boldsymbol{V}} - \boldsymbol{U}_j^T \bar{\boldsymbol{T}}_V\right) \mathrm{d}\partial\Omega + \boldsymbol{C}_j^T \bar{\boldsymbol{V}}(P_0)\end{aligned} \tag{25}$$

$$\begin{aligned}\boldsymbol{C}_j^T \boldsymbol{U}(P_0) = {}& \int_{\partial\Omega_{\langle k\rangle}} \left(\boldsymbol{U}_j^T \boldsymbol{T}_U - \boldsymbol{T}_j^T \boldsymbol{U}\right) \mathrm{d}\partial\Omega \\ & + \int_{\Omega_{\langle k\rangle}} \boldsymbol{U}_j^T \left(\mathcal{D}_x^T \boldsymbol{R}\boldsymbol{I}_z + \boldsymbol{I}_z^T \boldsymbol{R}\mathcal{D}_x\right)(\boldsymbol{V} - \bar{\boldsymbol{V}})\, \mathrm{d}\Omega \\ & - \int_{\partial\Omega_{\langle k\rangle}} \boldsymbol{U}_j^T \mathcal{D}_{xn}^T \boldsymbol{R}\boldsymbol{I}_z (\boldsymbol{V} - \bar{\boldsymbol{V}})\, \mathrm{d}\Omega \\ & + \int_{\partial\Omega_{\langle k\rangle}} \left(\boldsymbol{T}_j^T \bar{\boldsymbol{U}} - \boldsymbol{U}_j^T \bar{\boldsymbol{T}}_U\right) \mathrm{d}\partial\Omega + \boldsymbol{C}_j^T \bar{\boldsymbol{U}}(P_0)\end{aligned} \tag{26}$$

where $\bar{\boldsymbol{T}}_V$ and $\bar{\boldsymbol{T}}_U$ are the generalized boundary tractions corresponding to $\bar{\boldsymbol{V}}$ and $\bar{\boldsymbol{U}}$, respectively.

V. Boundary Integral Equations

Writing the boundary integral representation given by Eqs. (25) and (26) for four independent fundamental solutions, related to four independent electromechanical load conditions, one obtains the matrix form of the Somigliana identity for piezoelectric beam-type structures giving the three displacement components and electric potential at P_0. One has

$$\begin{aligned}\boldsymbol{C}^* \boldsymbol{V}(P_0) = {}& \int_{\partial\Omega_{\langle k\rangle}} \left(\boldsymbol{U}^* \boldsymbol{T}_V - \boldsymbol{T}^* \boldsymbol{V}\right) \mathrm{d}\partial\Omega \\ & + \int_{\partial\Omega_{\langle k\rangle}} \left(\boldsymbol{T}^* \bar{\boldsymbol{V}} - \boldsymbol{U}^* \bar{\boldsymbol{T}}_V\right) \mathrm{d}\partial\Omega + \boldsymbol{C}^* \bar{\boldsymbol{V}}(P_0)\end{aligned} \tag{27}$$

$$\begin{aligned}\boldsymbol{C}^* \boldsymbol{U}(P_0) = {}& \int_{\partial\Omega_{\langle k\rangle}} \left(\boldsymbol{U}^* \boldsymbol{T}_U - \boldsymbol{T}^* \boldsymbol{U}\right) \mathrm{d}\partial\Omega \\ & + \int_{\Omega_{\langle k\rangle}} \boldsymbol{U}^* \left(\mathcal{D}_x^T \boldsymbol{R}\boldsymbol{I}_z + \boldsymbol{I}_z^T \boldsymbol{R}\mathcal{D}_x\right)(\boldsymbol{V} - \bar{\boldsymbol{V}})\, \mathrm{d}\Omega \\ & - \int_{\partial\Omega_{\langle k\rangle}} \boldsymbol{U}^* \mathcal{D}_{xn}^T \boldsymbol{R}\boldsymbol{I}_z (\boldsymbol{V} - \bar{\boldsymbol{V}})\, \mathrm{d}\Omega \\ & + \int_{\partial\Omega_{\langle k\rangle}} \left(\boldsymbol{T}^* \bar{\boldsymbol{U}} - \boldsymbol{U}^* \bar{\boldsymbol{T}}_U\right) \mathrm{d}\partial\Omega + \boldsymbol{C}^* \bar{\boldsymbol{U}}(P_0)\end{aligned} \tag{28}$$

In the preceding relations, one has to set $\boldsymbol{U}^* = [U_{ij}]^T$ and $\boldsymbol{T}^* = [T_{ij}]^T$, where U_{ij} and T_{ij} indicate the ith component of generalized displacements and tractions of the jth fundamental solution, respectively. A useful expression for the matrix of the coefficients $\boldsymbol{C}^*$ is accomplished by specialization of Eqs. (27) and (28) for a constant generalized displacement field. By so doing, Eq. (27) is identically satisfied, whereas from Eq. (28) one obtains

$$\boldsymbol{C}^* = -\int_{\partial\Omega_{\langle k\rangle}} \boldsymbol{T}^*\, \mathrm{d}\partial\Omega \tag{29}$$

Equations (27) and (28) are valid for each internal point P_0 and then, setting P_0 on the boundary, through a suitable limit procedure,[46] they provide a system of integral equations whose solution with appropriate boundary conditions gives the generalized displacements and tractions on the boundary of the considered ply. Note that, for a ply within the laminate, some of the boundary conditions are supplied by the interface continuity conditions. Moreover, because of the behavior of the employed fundamental solution, when P_0 lies on the ply boundary, some kernels involved in the integral representation become singular, and then the relative integrals have to be considered in the sense of a Cauchy principal value.[46] The piezoelectric composite laminate model is attained by coupling the boundary integral equations of each ply by means of the interface continuity relations, namely, generalized displacements continuity and generalized tractions equilibrium. Because of the structure of the Somigliana identity for piezoelectric plies, this laminate model consists of two partially coupled sets of integral equations. The solution of the first set of integral equations directly provides the part of the piezoelastic response linearly varying along the laminate span. Once this part is determined, it can be substituted in the second set whose solution provides the along span constant part of the piezoelastic response. The analysis of Eqs. (27) and (28) shows that the proposed model reduces to a pure boundary model for piezoelectric composite laminates subjected to axial, bending, and twisting loadings, whereas for shear/bending loadings it entails domain integrals involving the field representation of $\boldsymbol{V}$ in terms of its boundary characteristics. This makes the present formulation more appealing for the implementation of discrete models for the analysis of piezoelectric laminates problems.

VI. Generalized Stresses Boundary Integral Representation

The generalized displacement boundary integral representation given by Eqs. (27) and (28) allows one to deduce the boundary integral representation for the stress field. By differentiation of Eqs. (27) and (28) with respect to P_0, and with the constitutive equations taken into account,[46] the generalized stresses of the kth ply are

$$\Sigma_V(P_0) = \int_{\partial\Omega_{\langle k\rangle}} \left\{ \Xi^*[\boldsymbol{V} - \bar{\boldsymbol{V}} + \bar{\boldsymbol{V}}(P_0)] - \boldsymbol{\Theta}^*[\boldsymbol{T}_V - \bar{\boldsymbol{T}}_V] \right\} \mathrm{d}\partial\Omega + \boldsymbol{R}_{\langle k\rangle}\boldsymbol{I}_z\boldsymbol{X}_2(P_0)\boldsymbol{k} \tag{30}$$

$$\Sigma_U(P_0) = \int_{\partial\Omega_{\langle k\rangle}} \left\{ \Xi^*[\boldsymbol{U} - \bar{\boldsymbol{U}} + \bar{\boldsymbol{U}}(P_0)] - \boldsymbol{\Theta}^*[\boldsymbol{T}_U - \bar{\boldsymbol{T}}_U] \right\} \mathrm{d}\partial\Omega - \int_{\Omega_{\langle k\rangle}} \boldsymbol{\Theta}^*\left[\mathcal{D}_x^T\boldsymbol{R}\boldsymbol{I}_z + \boldsymbol{I}_z^T\boldsymbol{R}\mathcal{D}_x\right](\boldsymbol{V} - \bar{\boldsymbol{V}})\,\mathrm{d}\Omega + \int_{\partial\Omega_{\langle k\rangle}} \boldsymbol{\Theta}^*\mathcal{D}_{xn}^T\boldsymbol{R}\boldsymbol{I}_z(\boldsymbol{V} - \bar{\boldsymbol{V}})\,\mathrm{d}\Omega + \boldsymbol{R}_{\langle k\rangle}\boldsymbol{I}_z[\boldsymbol{V}(P_0) + \boldsymbol{X}_1(P_0)\boldsymbol{k}] \tag{31}$$

The kernels $\boldsymbol{\Theta}^*$ and Ξ^* are obtained by application of the operator $\boldsymbol{R}\mathcal{D}_x\boldsymbol{C}^{*-1}$ to $\boldsymbol{U}^*$ and $\boldsymbol{T}^*$, respectively. Once the boundary generalized displacements and tractions are determined, the boundary integral representations given by Eqs. (27), (28), (30) and (31) allow one to obtain the electromechanical response at any internal point of the laminate in a pointwise fashion.

VII. Numerical Model

The solution of the model of the piezoelectric laminate can be numerically achieved by the multidomain BEM. Following the classical boundary element approach,[46] the boundary $\partial\Omega_{\langle k\rangle}$ of each ply is discretized into n boundary elements denoted by $\partial\Omega^q_{\langle k\rangle}$ (Fig. 2). Over each of these elements, the generalized displacement functions and tractions are expressed as

$$\boldsymbol{V} = \mathcal{L}(\xi)\boldsymbol{V}^q_{\langle k\rangle} \tag{32}$$

$$\boldsymbol{T}_V = \mathcal{L}(\xi)\boldsymbol{T}^q_{V\langle k\rangle} \tag{33}$$

$$\boldsymbol{U} = \mathcal{L}(\xi)\boldsymbol{U}^q_{\langle k\rangle} \tag{34}$$

$$\boldsymbol{T}_U = \mathcal{L}(\xi)\boldsymbol{T}^q_{U\langle k\rangle} \tag{35}$$

where the vectors indicated by the notation $\boldsymbol{X}^q_{\langle k\rangle}$ collect the values of the quantity $\boldsymbol{X}$ at the nodes of the boundary element $\partial\Omega^q_{\langle k\rangle}$. In the preceding relationships, $\mathcal{L}(\xi)$ is the shape function matrix whose elements are one-dimensional interpolation functions defined with respect to the local nondimensional coordinate $\xi = \xi(P)$, with $0 \le \xi \le 1$ (Fig. 2). Additionally, the ply domain $\Omega_{\langle k\rangle}$ is divided into m internal cells of domain $\Omega^r_{\langle k\rangle}$, over which the following approximation of the displacement function $\boldsymbol{V}$ is assumed:

$$\boldsymbol{V} = \mathcal{F}(\xi_1, \xi_2)\tilde{\boldsymbol{V}}^r_{\langle k\rangle} \tag{36}$$

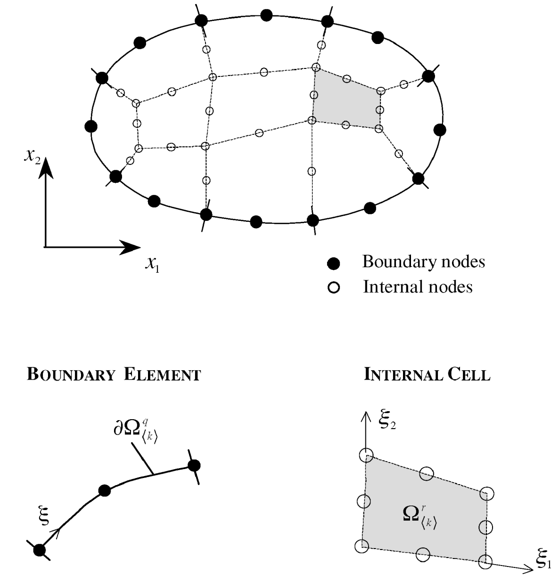

Fig. 2 Boundary element discretization and reference systems.

In Eq. (36), the vector $\tilde{\boldsymbol{V}}^r_{\langle k\rangle}$ collects the values of $\boldsymbol{V}$ at the nodes of the cell $\Omega^r_{\langle k\rangle}$, and $\mathcal{F}(\xi_1, \xi_2)$ is the shape function matrix whose elements are two-dimensional interpolation functions defined with respect to the local coordinates $\xi_\alpha = \xi_\alpha(P)$, where $\alpha = 1, 2$ and $0 \le \xi_\alpha \le 1$ (Fig. 2). No limitations are imposed on the order of the interpolation functions for the generalized displacement functions and tractions. Anyway, to preserve the model consistency, the two-dimensional shape functions for the approximation of the displacement functions $\boldsymbol{V}$ in the inner region should be suitably chosen to ensure the interelement continuity in the domain and between the boundary and the domain. With these assumptions, the discretized form of Eq. (27) for any point P_i of the kth ply is obtained by substitution of the expressions (32) and (33). This results in the following relation:

$$\boldsymbol{C}^*_{ii}\boldsymbol{V}(P_i) + \sum_{q=1}^{n}\hat{\boldsymbol{H}}_{iq}\boldsymbol{V}^q_{\langle k\rangle} + \sum_{q=1}^{n}\boldsymbol{G}_{iq}\boldsymbol{T}^q_{V\langle k\rangle} = \sum_{q=1}^{n}\boldsymbol{B}_{iq} \tag{37}$$

In the preceding equation, the influence coefficients and the right-hand side are defined by

$$\hat{\boldsymbol{H}}_{iq} = \int_0^1 \boldsymbol{T}^*(P(\xi), P_i)\mathcal{L}(\xi)J^q(\xi)\,\mathrm{d}\xi \tag{38}$$

$$\boldsymbol{G}_{iq} = -\int_0^1 \boldsymbol{U}^*(P(\xi), P_i)\mathcal{L}(\xi)J^q(\xi)\,\mathrm{d}\xi \tag{39}$$

$$\boldsymbol{B}_{iq} = \int_0^1 \left\{ \boldsymbol{T}^*(P(\xi), P_i)[\bar{\boldsymbol{V}}(P(\xi)) - \bar{\boldsymbol{V}}(P_i)] - \boldsymbol{U}^*(P(\xi), P_i)\bar{\boldsymbol{T}}_V(P(\xi)) \right\} J^q(\xi)\,\mathrm{d}\xi \tag{40}$$

where J^q is the Jacobian of the transformation from the global coordinates x_j, $j = 1, 2$, to the local reference system ξ of the boundary element $\partial\Omega^q_{\langle k\rangle}$. The coefficients $\boldsymbol{C}^*_{ii}$ are obtained from the discretized form of the Eq. (29):

$$\boldsymbol{C}^*_{ii} = -\sum_{q=1}^{n}\int_0^1 \boldsymbol{T}^*(P(\xi), P_i)J^q(\xi)\,\mathrm{d}\xi \tag{41}$$

By taking the field point P_i to all of the boundary nodes and absorbing the $\boldsymbol{C}^*_{ii}$ matrix with the corresponding block of $\hat{\boldsymbol{H}}_{ii}$ (Ref. 46), one obtains a linear algebraic system that can be compactly written as

$$\boldsymbol{H}_{\langle k\rangle}\boldsymbol{\Delta}_{V\langle k\rangle} + \boldsymbol{G}_{\langle k\rangle}\boldsymbol{P}_{V\langle k\rangle} = \boldsymbol{B}_{\langle k\rangle} \tag{42}$$

where $\boldsymbol{H}_{\langle k\rangle}$ and $\boldsymbol{G}_{\langle k\rangle}$ are the square influence matrices constructed block by block from the relationships (38), (39), and (41). $\boldsymbol{B}_{\langle k\rangle}$ is the right-hand side assembled by the use of Eq. (40), $\boldsymbol{\Delta}_{V\langle k\rangle}$ is the vector containing the nodal values of $\boldsymbol{V}$, and $\boldsymbol{P}_{V\langle k\rangle}$ is the vector of the nodal values of $\boldsymbol{T}_V$ for the kth ply. Analogously, by the use of Eqs. (34–36), the discretized version of Eq. (28) becomes

$$\boldsymbol{C}^*_{ii}\boldsymbol{U}(P_i) + \sum_{q=1}^{n}\hat{\boldsymbol{H}}_{iq}\boldsymbol{U}^q_{\langle k\rangle} + \sum_{q=1}^{n}\boldsymbol{G}_{iq}\boldsymbol{T}^q_{U\langle k\rangle} = \sum_{j=1}^{q}\boldsymbol{Q}_{iq}\boldsymbol{V}^q_{\langle k\rangle} + \sum_{r=1}^{m}\boldsymbol{W}_{ir}\tilde{\boldsymbol{V}}^r_{\langle k\rangle} + \sum_{q=1}^{n}\boldsymbol{Y}_{iq} + \sum_{r=1}^{m}\boldsymbol{K}_{ir} \tag{43}$$

The coefficients involved in the preceding equation are defined as follows:

$$\boldsymbol{Q}_{iq} = -\int_0^1 \boldsymbol{U}^*(P(\xi), P_i)\mathcal{D}^T_{xn}\boldsymbol{R}\boldsymbol{I}_z\mathcal{L}(\xi)J^q(\xi)\,\mathrm{d}\xi \tag{44}$$

$$\boldsymbol{W}_{ir} = \int_0^1\int_0^1 \boldsymbol{U}^*(P(\xi_1,\xi_2), P_i)\big[\mathcal{D}^T_\xi\boldsymbol{R}\boldsymbol{I}_z + \boldsymbol{I}^T_z\boldsymbol{R}\mathcal{D}_\xi\big] \times \mathcal{F}(\xi_1,\xi_2)J^r(\xi_1,\xi_2)\,\mathrm{d}\xi_1\,\mathrm{d}\xi_2 \tag{45}$$

$$\boldsymbol{Y}_{iq} = \int_0^1 \big\{\boldsymbol{T}^*(P(\xi), P_i)[\bar{\boldsymbol{U}}(P(\xi)) - \bar{\boldsymbol{U}}(P_0)] - \boldsymbol{U}^*(P(\xi), P_i)\big[\bar{\boldsymbol{T}}_U(P(\xi)) - \mathcal{D}^T_{xn}\boldsymbol{R}\boldsymbol{I}_z\bar{\boldsymbol{V}}(P(\xi))\big]\big\}J^q(\xi)\,\mathrm{d}\xi \tag{46}$$

$$\boldsymbol{K}_{ir} = -\int_0^1\int_0^1 \boldsymbol{U}^*(P(\xi_1,\xi_2), P_i)\big[\mathcal{D}^T_\xi\boldsymbol{R}\boldsymbol{I}_z + \boldsymbol{I}^T_z\boldsymbol{R}\mathcal{D}_\xi\big] \times \bar{\boldsymbol{V}}(P(\xi_1,\xi_2), P_i)J^r(\xi_1,\xi_2)\,\mathrm{d}\xi_1\,\mathrm{d}\xi_2 \tag{47}$$

where the operator $\mathcal{D}_\xi$ is obtained by expression of the elements of the operator $\mathcal{D}_x$ in terms of the local coordinate system. Moreover, the notation $J^r(\xi_1, \xi_2)$ indicates the Jacobian of the transformation from the global coordinate x_j, $j = 1, 2$, to the local system ξ_j, $j = 1, 2$, of the internal cell $\Omega^r_{\langle k\rangle}$. Collocating Eq. (43) at the boundary nodes, one obtains the following linear algebraic system:

$$\boldsymbol{H}_{\langle k\rangle}\boldsymbol{\Delta}_{U\langle k\rangle} + \boldsymbol{G}_{\langle k\rangle}\boldsymbol{P}_{U\langle k\rangle} = \boldsymbol{Q}_{\langle k\rangle}\boldsymbol{\Delta}_{V\langle k\rangle} + \boldsymbol{W}_{\langle k\rangle}\boldsymbol{\delta}_{V\langle k\rangle} + \boldsymbol{Y}_{\langle k\rangle} + \boldsymbol{K}_{\langle k\rangle} \tag{48}$$

where $\boldsymbol{\Delta}_{U\langle k\rangle}$ and $\boldsymbol{P}_{U\langle k\rangle}$ are the vectors containing the nodal values of $\boldsymbol{U}$ and $\boldsymbol{T}_U$ of the kth ply, respectively. The matrices appearing on the right-hand side of Eq. (48) are constructed on the basis of Eqs. (44–47) by the standard assembling procedure.[46] The vector $\boldsymbol{\delta}_{V\langle k\rangle}$ collects all of the values of $\boldsymbol{V}$ at the cell nodal points of the kth ply. It can be calculated with the generalized displacement boundary integral representation, then, by collocation of Eq. (37) at the cell nodal points, one has

$$\boldsymbol{\delta}_{V\langle k\rangle} = \tilde{\boldsymbol{G}}_{\langle k\rangle}\boldsymbol{P}_{V\langle k\rangle} + \tilde{\boldsymbol{H}}_{\langle k\rangle}\boldsymbol{\Delta}_{V\langle k\rangle} + \tilde{\boldsymbol{B}}_{\langle k\rangle} \tag{49}$$

with the obvious meaning of the symbols. By the use of Eq. (49), the system given by Eq. (48) is rewritten in terms of boundary variables as

$$\boldsymbol{H}_{\langle k\rangle}\boldsymbol{\Delta}_{U\langle k\rangle} + \boldsymbol{G}_{\langle k\rangle}\boldsymbol{P}_{U\langle k\rangle} = \big(\boldsymbol{Q}_{\langle k\rangle} + \boldsymbol{W}_{\langle k\rangle}\tilde{\boldsymbol{H}}_{\langle k\rangle}\big)\boldsymbol{\Delta}_{V\langle k\rangle} + \boldsymbol{W}_{\langle k\rangle}\tilde{\boldsymbol{G}}_{\langle k\rangle}\boldsymbol{P}_{V\langle k\rangle} + \boldsymbol{W}_{\langle k\rangle}\tilde{\boldsymbol{B}}_{\langle k\rangle} + \boldsymbol{Y}_{\langle k\rangle} + \boldsymbol{K}_{\langle k\rangle} \tag{50}$$

The resolving system for the whole laminate follows when Eqs. (42) and (50), written for all of the plies of the laminate, are coupled, through the interface continuity conditions, and then by enforcement of the external boundary conditions, for example, the condition of zero boundary tractions on the laminate external surfaces. For a bonding interface $\partial\Omega_{mn}$ between the mth and the nth ply, the discrete form of the continuity conditions can be written as

$$\boldsymbol{C}_{mn}\boldsymbol{\Delta}_{J\langle m\rangle} = \boldsymbol{C}_{nm}\boldsymbol{\Delta}_{J\langle n\rangle} \qquad \text{for} \qquad J = V, U \tag{51}$$

$$\boldsymbol{C}_{mn}\boldsymbol{P}_{J\langle m\rangle} = -\boldsymbol{C}_{nm}\boldsymbol{P}_{J\langle n\rangle} \qquad \text{for} \qquad J = V, U \tag{52}$$

where the matrices $\boldsymbol{C}_{mn}$ are suitably constructed to select the nodal values of the mth ply boundary, which belong to the interface $\partial\Omega_{mn}$. With the same notation, the boundary condition for the external surfaces of the mth ply can be written as

$$\boldsymbol{C}^D_{mm}\boldsymbol{V}_{\langle m\rangle} + \boldsymbol{C}^P_{mm}\boldsymbol{P}_{V\langle m\rangle} = \bar{\boldsymbol{q}}_V \tag{53}$$

$$\boldsymbol{C}^D_{mm}\boldsymbol{U}_{\langle m\rangle} + \boldsymbol{C}^P_{mm}\boldsymbol{P}_{U\langle m\rangle} = \bar{\boldsymbol{q}}_U \tag{54}$$

where overbarred vectors denote prescribed quantities, and the matrices $\boldsymbol{C}^D_{mm}$ and $\boldsymbol{C}^P_{mm}$ are suitably constructed to select the nodal generalized displacements and tractions at nodes belonging to the external surface of the ply, respectively. Bear in mind that N is the number of plies; the boundary discretized model of the piezoelectric composite laminate is, therefore, given by Eqs. (42) and (50), written for $k = 1, 2, \ldots, N$; Eqs. (51) and (52), written for $m = 1, 2, \ldots, N$ and $n = m+1, m+2, \ldots, N$; and, finally, by Eqs. (53) and (54) written for $k = 1, 2, \ldots, N$. Thus, all of the equilibrium equations, interface continuity conditions, and boundary conditions are satisfied, and the numerical solution obtained is, therefore, consistent. As just pointed out, the laminate model consists of a set of partially coupled equations. Its solution can, therefore, be achieved as described in the following:

1) The system given by Eq. (42), written for $k = 1, 2, \ldots, N$; Eqs. (51) and (52), written for $J = V$, $m = 1, 2, \ldots, N$, and $n = m+1, m+2, \ldots, N$; and Eq. (53), written for $k = 1, 2, \ldots, N$, is solved for $\boldsymbol{\Delta}_V$ and $\boldsymbol{P}_V$.

2) On substitution of $\boldsymbol{\Delta}_V$, the system given by Eq. (50), written for $k = 1, 2, \ldots, N$; Eqs. (51) and (52), written for $J = U$, $m = 1, 2, \ldots, N$, and $n = m+1, m+2, \ldots, N$; and Eq. (54), written for $k = 1, 2, \ldots, N$, is solved for $\boldsymbol{\Delta}_U$ and $\boldsymbol{P}_U$.

Moreover, if the laminate has a classical configuration and presents only one interface between contiguous plies, very efficient solution schemes can be employed for the model solution as described in Ref. 37. Note that when the laminate is subjected to axial extension, bending, and torsion, the generalized displacement function $\boldsymbol{V}$ and the associated generalized tractions $\boldsymbol{T}_V$ are zero, and the ply governing equations reduce to

$$\boldsymbol{H}_{\langle k\rangle}\boldsymbol{\Delta}_{U\langle k\rangle} + \boldsymbol{G}_{\langle k\rangle}\boldsymbol{P}_{U\langle k\rangle} = \boldsymbol{Y}_{\langle k\rangle} \tag{55}$$

The laminate response can, therefore, be obtained by direct solution of the system given by Eq. (55), written for $k = 1, 2, \ldots, N$; Eqs. (51) and (52), written for $J = U$, $m = 1, 2, \ldots, N$, and $n = m+1, m+2, \ldots, N$; and Eq. (53), written for $k = 1, 2, \ldots, N$. The quantities characterizing the piezoelastic response at laminate internal points, namely, generalized displacements and stresses, are computed by the use of the discretized form of the corresponding boundary integral representation. These expressions can be deduced following the method proposed for the discretization of the boundary integral equations,[46] and they are not rewritten here for the sake of conciseness.

VIII. Numerical Results and Discussion

To investigate the performances of the proposed approach and point out its features, a computer code has been developed to calculate piezoelectric laminate electromechanical response. The computer code allows consideration of general layups and section geometries, and it was implemented with the following major attributes. Straight elements are employed for the cross section boundary discretization, and linear interpolation of the unknown data is assumed over each boundary element. For the internal cells, isoparametric four-node elements are used. The influence coefficients are numerically computed by the use of standard Gaussian quadrature, coupled with an adaptive integration scheme that allows the kernel singularities to be taken into account.[47] In particular, eight-point, one-dimensional Gaussian quadrature has been used to perform integrations over the boundary elements, whereas 16-point, two-dimensional Gaussian quadrature has been employed for the domain integration over the cells. The interface continuity conditions are enforced, detecting automatically the boundaries common to contiguous plies by means of an interface identification algorithm.[45] To

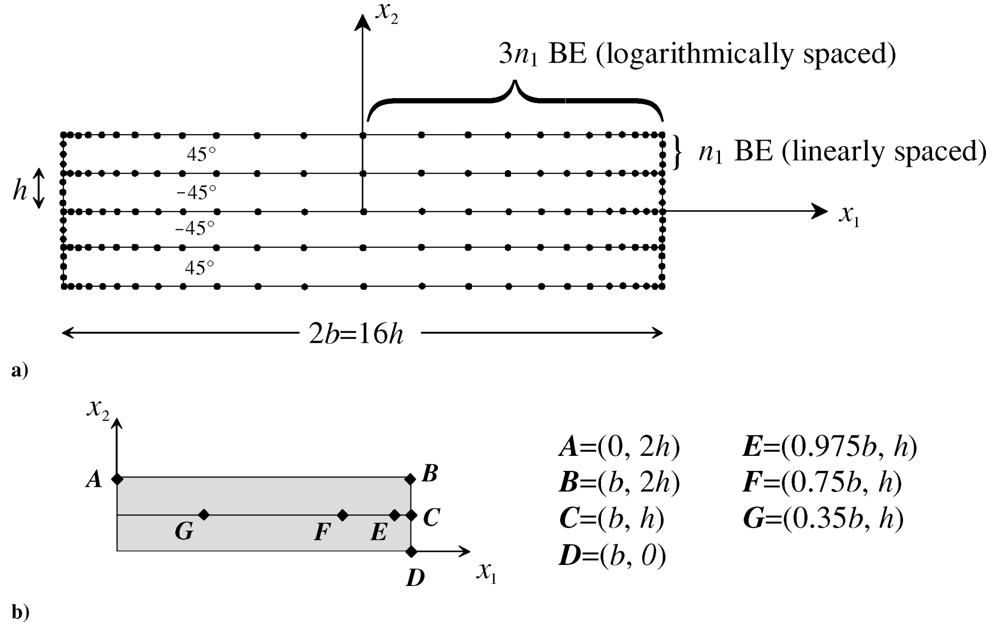

Fig. 3 Laminate discretization scheme.

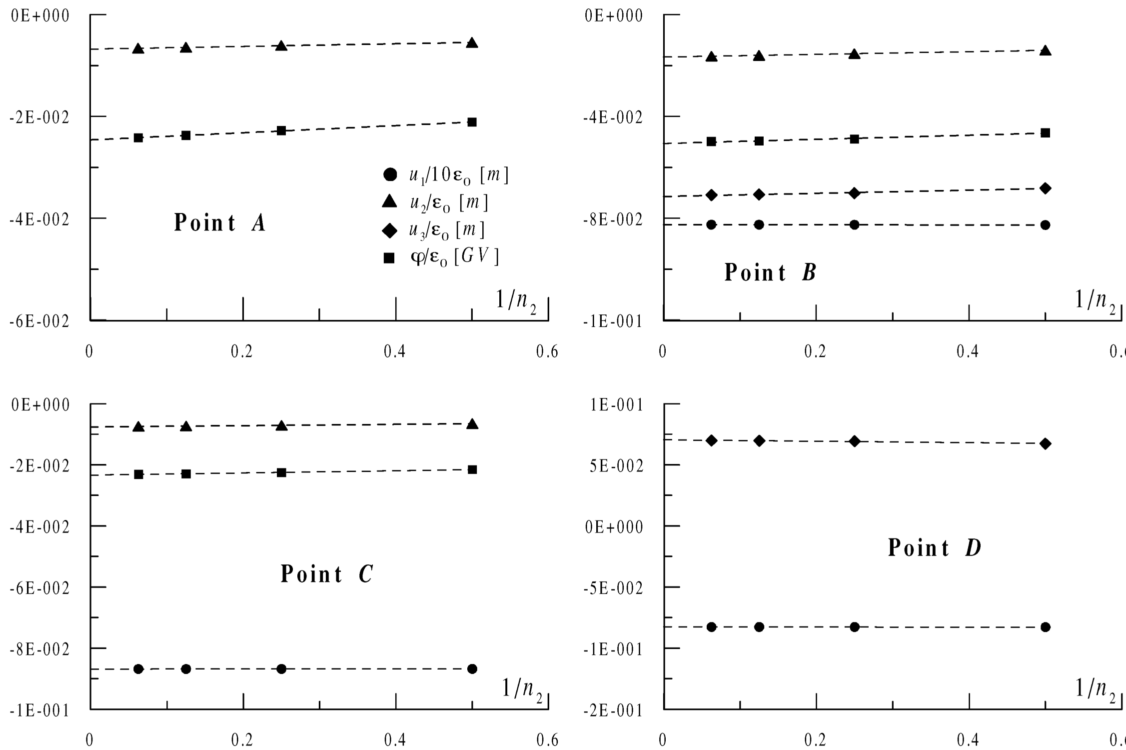

Fig. 4 Convergence curves for the generalized displacements of the [45/−45 deg]$_S$ PVDF laminate under axial extension.

ascertain the capabilities of the method, a convergence study has been performed to assess the characteristics for a correct boundary element modeling of the laminate cross section. This study was carried out for a typical four-ply [45/−45 deg]$_s$ symmetric laminate subjected to axial extension; each ply of the considered laminate has thickness h and width 16h and material properties corresponding to those of polyvinylidene fluoride (PVDF), which are given in Ref. 48. The discretization scheme employed is shown in Fig. 3a, where the mesh parameter n_1 is defined. The convergence curves for the generalized displacements and tractions at the locations denoted by capital letters in Fig. 3b are shown in Figs. 4 and 5 for different mesh refinements obtained by variation of n_1. The generalized displacements show a linear convergence for all of the points considered. As regards the generalized interlaminar stresses, note that they show linear convergence for points sufficiently far from the free edge, whereas at the free edge no convergence value seems to be reached. The singular behavior at the free edge is able to explain the deviation from linear convergence in the stresses near the free edge when these quantities are computed by the use of standard boundary elements with linear interpolation functions. However, as regards the accuracy of the solution in the region closely contiguous to the free edge, previous analysis of singular stress fields by numerical methods have shown the ability of the finite element method[49] and boundary element method[34] to capture successfully the steep gradients occurring in the structural response under these conditions. The convergence considerations pointed out for the case of

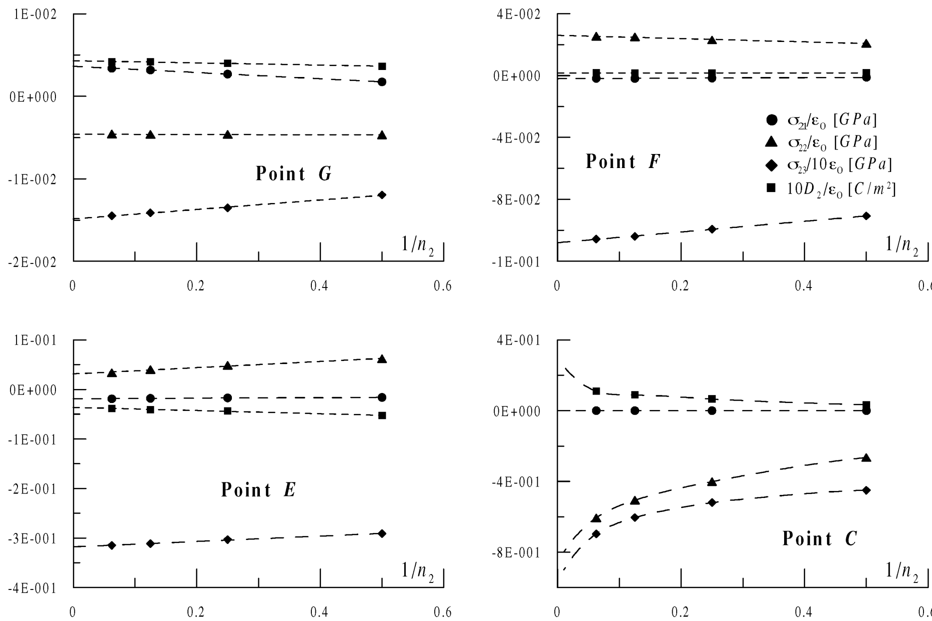

Fig. 5 Convergence curves for the generalized tractions of the [45/−45 deg]$_S$ PVDF laminate under axial extension.

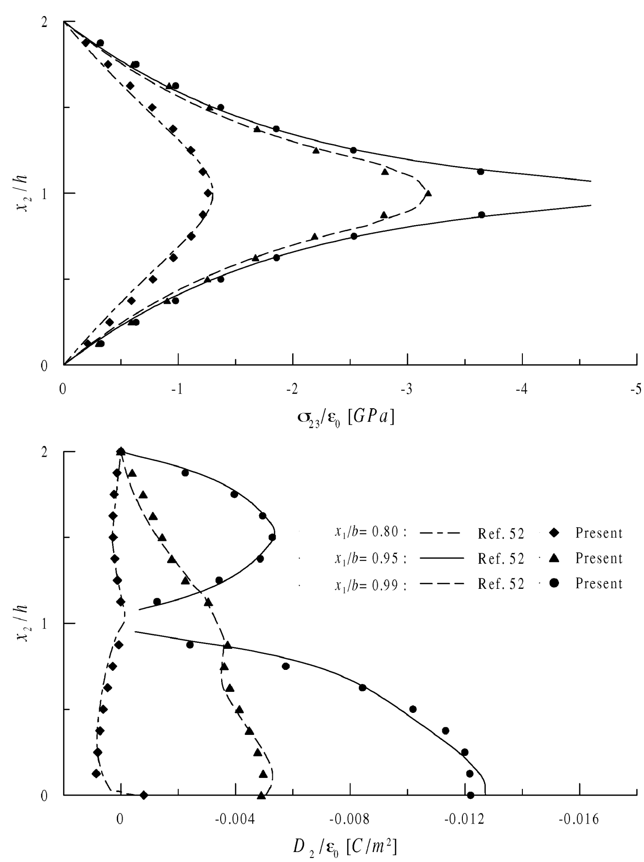

Fig. 6 Through-thickness distribution of the generalized interlaminar stresses σ_{23} and D_2 of the [45/−45 deg]$_S$ PVDF laminate under axial extension.

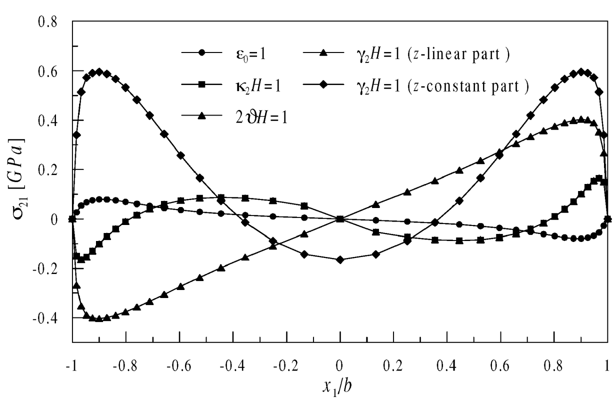

Fig. 7 Top interface $x_2 = h$ distribution of the interlaminar stress σ_{21} for the [45/−45 deg]$_S$ PVDF laminate under mechanical load conditions.

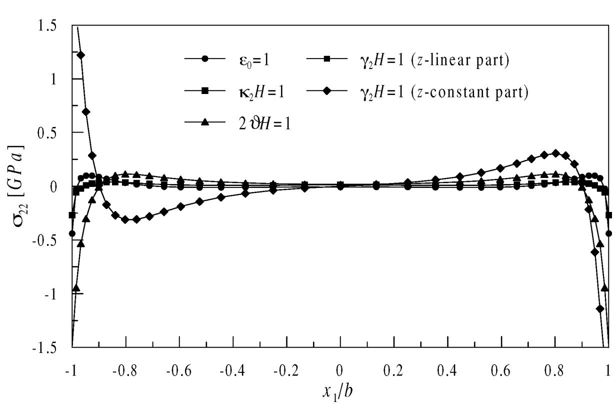

Fig. 8 Top interface $x_2 = h$ distribution of the interlaminar stress σ_{22} for the [45/−45 deg]$_S$ PVDF laminate under mechanical load conditions.

axial extension can be replicated for the other loading conditions because the mathematical structure of the resolving system maintains the same characteristics for the different loading conditions.

To asses the accuracy of the computed solution, the results obtained for $n_1 = 8$ have been compared with those recently obtained by an ad hoc approach, which is based on the use of generalized stress functions that provide a resolving system whose solution is obtained by an eigenfunction expansion method coupled with a boundary collocation technique.[50–52] A comparison of the through-thickness distributions of the interlaminar generalized stresses σ_{23} and D_2 is shown in Fig. 6. The agreement between the two solutions is good, proving that the present approach can accurately describe the electromechanical response of piezoelectric laminates. In addition, these results prove the effectiveness of the boundary integral approach, which is able to give accurate results of the free edge boundary layer with rather coarse meshes. Once the properties of the method have been ascertained, the basic characteristics of the electromechanical response in piezoelectric composite laminates can be analyzed. To point out the features of the laminate behavior, many angle-ply laminates with different stacking sequences and width-to-thickness ratios have been analyzed. In the following, only some results are presented to illustrate the piezoelastic response of laminates subjected to both mechanical and electrical loadings. In particular, representative results are given for the $[45/-45\ \mathrm{deg}]_S$ angle-ply laminate just described. The solutions obtained are presented and discussed in terms of interlaminar generalized stress distributions, which are a crucial topic for a comprehensive knowledge of the mechanisms and phenomena involved in piezoelectric laminate behavior.

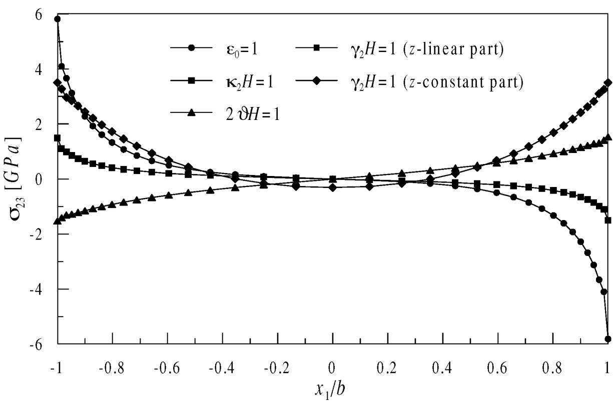

Fig. 9 Top interface $x_2 = h$ distribution of the interlaminar stress σ_{23} for the $[45/-45\ \mathrm{deg}]_S$ PVDF laminate under mechanical load conditions.

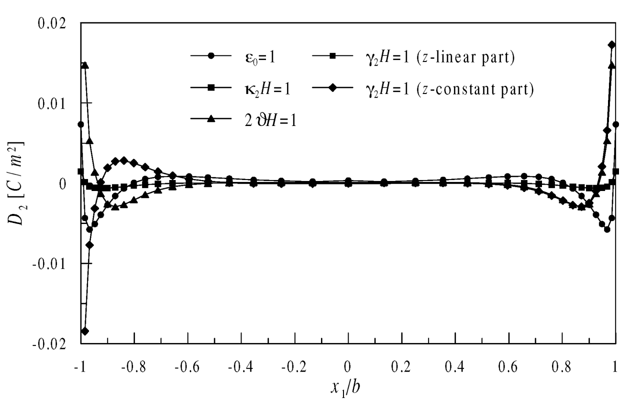

Fig. 10 Top interface $x_2 = h$ distribution of the interlaminar electric displacement D_2 for the $[45/-45\ \mathrm{deg}]_S$ PVDF laminate under mechanical load conditions.

Figures 7–10 show the interlaminar generalized stresses along the top interface $x_2 = h$ of the laminate subjected to mechanical loading. The analysis of these results, which are illustrative for the whole class of investigated laminates under mechanical loading, shows, as expected, an important edge effect for both mechanical and electric quantities. The distributions of generalized stresses and deformation are inherently three-dimensional. They cannot be determined accurately by extensions of the classical lamination theory, nor by approximate methods, which do not explicitly take the boundary-layer effect into account. The performed analyses show that the generalized stress distortion near the free edge decays with the distance from the edge, and the results for angle-ply laminates with plies having width-to-thickness ratios varying from 4 to 32 indicate that the region of disturbance is practically restricted to a width equal to the laminate thickness. This conclusion, previously found for classical composite laminates,[51] can, therefore, be extended to piezoelectric composite laminates. The interlaminar generalized stress distributions confirm the presence of a stress singularity like that found in classical composite laminates.[50] In addition, a free edge, singularity can be presumed for the electric displacement field, which can lead to reach a polarization saturation limit or trouble the electromechanical coupling characteristics. These phenomena should assume a great importance in the development of damage theories and control approaches for piezoelectric composite laminates. They can be quantitatively assessed by the present method, which is able to characterize the free edge singularity in terms of its power and strength, as shown earlier for classical composite laminates.[34]

Figure 11 shows the interlaminar generalized stress patterns for the laminate subjected to an electric load given by the electric potential Φ_0 applied on the upper surface of the laminate, and the electric potential $-\Phi_0$ applied on the lower surface of the laminate. Zero mechanical load $\boldsymbol{P}$ is applied at the laminate ends. With this load, the piezoelectric laminate experiences an axial deformation $\varepsilon_0/\Phi_0 = 3.57 \times 10^{-4}$ [1/GV], a bending curvature $\kappa_2/\Phi_0 = -2.76 \times 10^{-4}$ [1/m · GV], and a twisting $\vartheta/\Phi_0 = -1.12 \times 10^{-5}$ [1/m · GV], which are the fundamental parameters used to exert shape control of the laminate by means of its electromechanical coupling. Moreover the electromechanical response for this electric loading practically shares the same basic characteristics with the piezoelectric response of laminates mechanically loaded. In particular, the electric load generates a boundary layer in the stress field that should be used to control damage phenomena induced in the free edge regions by other kind of loads. These considerations can be also extended to other forms of the electric load, which are able to exert more complex deformation on the structure. In summary, the performed analyses suggest the possibility of the design of an effective control on the structural behavior of piezoelectric laminates by means of their inherent electromechanical coupling.

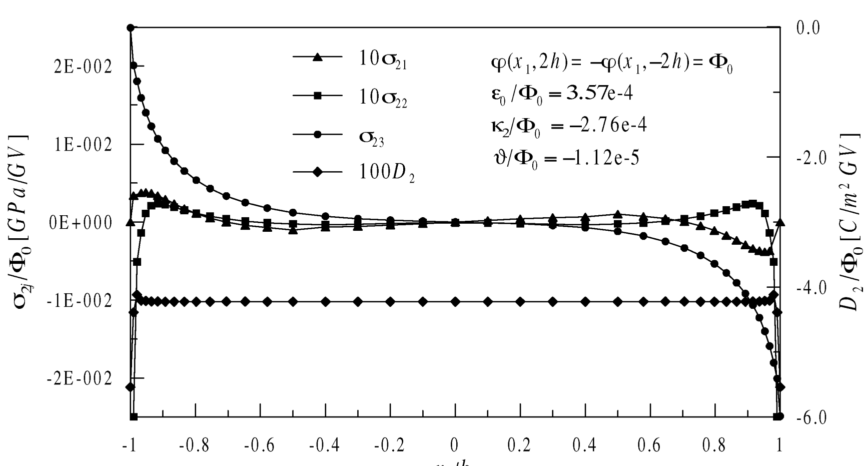

Fig. 11 Top interface $x_2 = h$ distribution of the generalized interlaminar stresses for the $[45/-45\ \mathrm{deg}]_S$ PVDF laminate under electrical load.

IX. Conclusions

A boundary integral representation of the solution of piezoelectric composite laminates subjected to axial extension, bending, twisting, shear/bending, and electric loadings has been presented. The approach is based on the electromechanical generalized variables, and it provides the model describing the behavior of each ply within the laminate in terms of two partially coupled integral identities for the generalized displacements. The model of the laminate as a whole is obtained from the plies integral equations accounting for the electromechanical interface continuity conditions. The approach proposed has some appealing features that are summarized as follows:

The formulation has been developed with full electromechanical coupling taken into account, and then it encompasses the related influences on the laminate structural and electrical behavior. The boundary integral representation for generalized displacements and stresses allows the determination of the laminate response in a pointwise fashion, preserving the inherent description of the electromechanical state. These model properties allow the use of the present formulation to investigate the characteristic features of piezoelectric composite behavior, addressing accurately boundary-layer and local phenomena. Moreover, the formulation is very well suited for the numerical implementation by the multidomain BEM with the related computational advantages. Numerical results have been presented and discussed. In conclusion, the solutions analyzed can be considered capable to model effectively the piezoelastic behavior, and they have shown the basic characteristics of piezoelectric composite laminate structural behavior.

Appendix: Particular Solution

A particular field solution $\bar{\boldsymbol{S}}$ of the ply governing equations is sought in the form of second-order polynomials. One writes

$$\bar{\boldsymbol{V}} = \boldsymbol{\Lambda a} \tag{A1}$$

$$\bar{\boldsymbol{U}} = \boldsymbol{\Lambda b} \tag{A2}$$

where $\boldsymbol{a}$ and $\boldsymbol{b}$ are (24×1) vectors containing the polynomial coefficients and $\boldsymbol{\Lambda}$ is defined as

$$\boldsymbol{\Lambda} = \boldsymbol{\Lambda}_1 x_1^2 + \boldsymbol{\Lambda}_2 x_2^2 + \boldsymbol{\Lambda}_3 x_1 x_2 + \boldsymbol{\Lambda}_4 x_1 + \boldsymbol{\Lambda}_5 x_2 + \boldsymbol{\Lambda}_6 \tag{A3}$$

The $\boldsymbol{\Lambda}_k$ are (4×24) matrices whose elements $\boldsymbol{\Lambda}_{kij}$ are given by

$$\begin{aligned} \boldsymbol{\Lambda}_{kij} &= 1 \qquad \text{for} \quad i = 1, 2, 3, 4, \qquad j = 6(i-1) + k \\ \boldsymbol{\Lambda}_{kij} &= 0 \qquad \text{otherwise} \end{aligned} \tag{A4}$$

With this choice of the particular solution, the compatibility conditions are identically satisfied, and then the coefficients $\boldsymbol{a}$ and $\boldsymbol{b}$ are obtained from the equilibrium equations. Setting

$$\mathcal{D} = \boldsymbol{I}_{x_1}\frac{\partial}{\partial x_1} + \boldsymbol{I}_{x_2}\frac{\partial}{\partial x_2} + \boldsymbol{I}_{x_3}\frac{\partial}{\partial x_3} = \boldsymbol{I}_{x_1}\frac{\partial}{\partial x_1} + \boldsymbol{I}_{x_2}\frac{\partial}{\partial x_2} + \boldsymbol{I}_{z}\frac{\partial}{\partial z} \tag{A5}$$

$$\tilde{\boldsymbol{A}}_{ij} = \boldsymbol{I}_{x_i}^T \boldsymbol{R} \boldsymbol{I}_{x_j} \tag{A6}$$

$$\boldsymbol{A}_{ij} = \tilde{\boldsymbol{A}}_{ij} + \tilde{\boldsymbol{A}}_{ij}^T \tag{A7}$$

from Eqs. (12) and (13), one has

$$\left[\frac{1}{2}\boldsymbol{A}_{11}\boldsymbol{\Lambda}_1 + \boldsymbol{A}_{12}\boldsymbol{\Lambda}_3 + \frac{1}{2}\boldsymbol{A}_{22}\boldsymbol{\Lambda}_2\right]\boldsymbol{a} + \left[\tilde{\boldsymbol{A}}_{13}\frac{\partial \boldsymbol{X}_2}{\partial x_1} + \tilde{\boldsymbol{A}}_{23}\frac{\partial \boldsymbol{X}_2}{\partial x_2}\right]\boldsymbol{k} = \boldsymbol{0} \tag{A8}$$

$$\begin{aligned} & x_1\left[(2\boldsymbol{A}_{13}\boldsymbol{\Lambda}_1 + \boldsymbol{A}_{23}\boldsymbol{\Lambda}_3)\boldsymbol{a} + \frac{1}{2}\boldsymbol{A}_{33}\frac{\partial \boldsymbol{X}_2}{\partial x_1}\boldsymbol{k}\right] \\ & + x_2\left[(\boldsymbol{A}_{13}\boldsymbol{\Lambda}_3 + 2\boldsymbol{A}_{23}\boldsymbol{\Lambda}_2)\boldsymbol{a} + \frac{1}{2}\boldsymbol{A}_{33}\frac{\partial \boldsymbol{X}_2}{\partial x_2}\boldsymbol{k}\right] \\ & + \left(\frac{1}{2}\boldsymbol{A}_{11}\boldsymbol{\Lambda}_1 + \boldsymbol{A}_{12}\boldsymbol{\Lambda}_3 + \frac{1}{2}\boldsymbol{A}_{22}\boldsymbol{\Lambda}_2\right)\boldsymbol{b} + (\boldsymbol{A}_{13}\boldsymbol{\Lambda}_4 + \boldsymbol{A}_{23}\boldsymbol{\Lambda}_5)\boldsymbol{a} \\ & + \left(\tilde{\boldsymbol{A}}_{13}\frac{\partial \boldsymbol{X}_1}{\partial x_1} + \tilde{\boldsymbol{A}}_{23}\frac{\partial \boldsymbol{X}_1}{\partial x_2}\right)\boldsymbol{k} = \boldsymbol{0} \end{aligned} \tag{A9}$$

By the equation of coefficients in the polynomial identity (A9), the preceding equations can be rewritten as

$$\begin{bmatrix} \frac{1}{2}\boldsymbol{A}_{11}\boldsymbol{\Lambda}_1 + \boldsymbol{A}_{12}\boldsymbol{\Lambda}_3 + \frac{1}{2}\boldsymbol{A}_{22}\boldsymbol{\Lambda}_2 & \boldsymbol{0} \\ 2\boldsymbol{A}_{13}\boldsymbol{\Lambda}_1 + \boldsymbol{A}_{23}\boldsymbol{\Lambda}_3 & \boldsymbol{0} \\ \boldsymbol{A}_{13}\boldsymbol{\Lambda}_3 + 2\boldsymbol{A}_{23}\boldsymbol{\Lambda}_2 & \boldsymbol{0} \\ \boldsymbol{A}_{13}\boldsymbol{\Lambda}_4 + \boldsymbol{A}_{23}\boldsymbol{\Lambda}_5 & \frac{1}{2}\boldsymbol{A}_{11}\boldsymbol{\Lambda}_1 + \boldsymbol{A}_{12}\boldsymbol{\Lambda}_3 + \frac{1}{2}\boldsymbol{A}_{22}\boldsymbol{\Lambda}_2 \end{bmatrix}$$

$$\times \begin{bmatrix} \boldsymbol{a} \\ \boldsymbol{b} \end{bmatrix} = -\begin{bmatrix} \left(\tilde{\boldsymbol{A}}_{13}\frac{\partial \boldsymbol{X}_2}{\partial x_1} + \tilde{\boldsymbol{A}}_{23}\frac{\partial \boldsymbol{X}_2}{\partial x_2}\right)\boldsymbol{k} \\ \frac{1}{2}\boldsymbol{A}_{33}\frac{\partial \boldsymbol{X}_2}{\partial x_1}\boldsymbol{k} \\ \frac{1}{2}\boldsymbol{A}_{33}\frac{\partial \boldsymbol{X}_2}{\partial x_2}\boldsymbol{k} \\ \left(\tilde{\boldsymbol{A}}_{13}\frac{\partial \boldsymbol{X}_1}{\partial x_1} + \tilde{\boldsymbol{A}}_{23}\frac{\partial \boldsymbol{X}_1}{\partial x_2}\right)\boldsymbol{k} \end{bmatrix} \tag{A10}$$

Then, by denotation by $\boldsymbol{K}$ and $\boldsymbol{Q}$ the matrix and the right-hand side of the system of algebraic equation (A10), respectively, a particular solution is determined by applying the least-square technique, and one has

$$\begin{bmatrix} \boldsymbol{a} \\ \boldsymbol{b} \end{bmatrix} = (\boldsymbol{K}^T\boldsymbol{K})^{-1}\boldsymbol{K}^T\boldsymbol{Q} \tag{A11}$$

References

[1] Crawley, E. F., and de Luis, J., "Use of Piezoelectric Actuators as Elements of Intelligent Structures," *AIAA Journal*, Vol. 25, No. 10, 1987, pp. 1373–1385.

[2] Crawley, E. F., "Intelligent Structures for Aerospace: A Technology Overview and Assessment," *AIAA Journal*, Vol. 32, No. 8, 1994, pp. 1689–1699.

[3] Noor, A. K., Venneri, S. L., Paul, D. B., and Hopkins, M. A., "Structure Technology for Future Aerospace Systems," *Computers and Structures*, Vol. 74, No. 5, 2000, pp. 507–519.

[4] Irschik, H., "A Review on Static and Dynamic Shape Control of Structures by Piezoelectric Actuation," *Engineering Structures*, Vol. 24, No. 1, 2002, pp. 5–11.

[5] Hagood, N. W., and Bent, A. A., "Development of Piezoelectric Fiber Composites for Structural Actuation," *Proceedings of the 34th AIAA/ASME/ASCE/AHS/ASC Structures, Structural Dynamics, and Materials Conference*, AIAA, Washington, DC, 1993, pp. 3625–3638.

[6] Lee, C. K., and Moon, F. C., "Modal Sensors/Actuators," *Journal of Applied Mechanics*, Vol. 57, No. 2, 1990, pp. 434–441.

[7] Crawley, E. F., and Lazarus, K. B., "Induced Strain Actuation of Isotropic and Anisotropic Plates," *AIAA Journal*, Vol. 29, No. 6, 1991, pp. 944–951.

[8] Wang, B. T., and Rogers, C. A., "Laminate Plate Theory for Spatially Distributed Induced Strain Actuators," *Journal of Composite Materials*, Vol. 25, No. 4, 1991, pp. 433–452.

[9] Heyliger, P., and Brooks, S., "Exact Solutions for Laminated Piezoelectric Plates in Cylindrical Bending," *Journal of Applied Mechanics*, Vol. 63, No. 4, 1996, pp. 903–910.

[10] Bisegna, P., and Maceri, F., "Exact Three-Dimensional Solution for Simply Supported Rectangular Piezoelectric Plates," *Journal of Applied Mechanics*, Vol. 63, No. 3, 1996, pp. 628–638.

[11] Heyliger, P., "Exact Solutions for Simply Supported Laminated Piezoelectric Plates," *Journal of Applied Mechanics*, Vol. 64, No. 2, 1997, pp. 299–306.

[12] Vel, S. S., and Batra, R. C., "Cylindrical Bending of Laminated Plates with Distributed and Segmented Piezoelectric Actuators/Sensors," *AIAA Journal*, Vol. 38, No. 5, 2000, pp. 857–867.

[13] Lee, J. S., and Jiang, L. Z., "Exact Electroelastic Analysys of Piezoelectric Laminae via State Space Approach," *International Journal of Solids and Structures*, Vol. 33, No. 7, 1996, pp. 977–990.

[14] Cheng, Z. Q., and Batra, R. C., "Three-Dimensional Asymptotic Analysis of Multiple Electroded Piezoelectric Laminates," *AIAA Journal*, Vol. 38, No. 2, 2000, pp. 317–324.

[15] Yang, S., and Ngoi, B., "Shape Control of Beams by Piezoelectric Actuators," *AIAA Journal*, Vol. 38, No. 12, 2000, pp. 2292–2298.

[16] Allik, H., and Hughes, T. J. R., "Finite Element Method for Piezoelectric Vibrations," *International Journal for Numerical Methods in Engineering*, Vol. 2, No. 2, 1970, pp. 151–157.

[17] Tzou, H. S., and Tseng, C. I., "Distributed Piezoelectric Sensor/Actuator Design for Dynamic Measurement/Control of Distributed Parameter Systems: A Piezoelectric Finite Element Approach," *Journal of Sound and Vibration*, Vol. 138, No. 1, 1990, pp. 17–34.

[18] Ha, S. K., Keilers, C., and Chang, F. K., "Finite Element Analysis of Composite Structures Containing Distributed Piezoceramic Sensors and Actuators," *AIAA Journal*, Vol. 30, No. 3, 1992, pp. 772–780.

[19] Benjeddou, A., "Advances in Piezoelectric Finite Element Modeling of Adaptive Structural Elements: A Survey," *Computers and Structures*, Vol. 76, No. 1–3, 2000, pp. 347–363.

[20] Robbins, D. H., and Reddy, J. N., "Analysis of Piezoelectrically Actuated Beams Using a Layer-Wise Displacement Theory," *Computers and Structures*, Vol. 41, No. 2, 1991, pp. 265–279.

[21] Robbins, D. H., and Reddy, J. N., "Modelling of Thick Composites Using a Layerwise Laminate Theory," *International Journal for Numerical Methods in Engineering*, Vol. 36, No. 4, 1993, pp. 655–677.

[22] Chandrashekhara, H., and Agarwal, A. N., "Active Vibration Control of Laminated Composites Plates Using Piezoelectric Devices: A Finite Element Approach," *Journal of Intelligent Materials, System and Structures*, Vol. 4, No. 10, 1993, pp. 496–508.

[23] Detwiler, D. T., Shen, M. H. H., and Venkayya, V. B., "Finite Element Analysis of Laminated Composite Structures Containing Distributed Piezoelectric Actuators and Sensors," *Finite Elements in Analysis and Design*, Vol. 20, No. 2, 1995, pp. 87–100.

[24] Saravanos, D. A., Heyliger, P. R., and Hopkins, D. A., "Layerwise Mechanics and Finite Element for the Dynamic Analysis of Piezoelectric Composite Plates," *International Journal of Solids and Structures*, Vol. 34, No. 26, 1997, pp. 3355–3371.

[25] Lee, H. J., and Saravanos, D. A., "Generalized Finite Element Formulation for Smart Multilayered Thermal Piezoelectric Composite Plates," *International Journal of Solids and Structures*, Vol. 34, No. 3, 1997, pp. 359–378.

[26] Varadarajan, S., Chandrashekhara, K., and Argawal, S., "Adaptive Shape Control of Laminated Composite Plates Using Piezoelectric Materials," *AIAA Journal*, Vol. 36, No. 9, 1998, pp. 1694–1698.

[27] Lee, J. S., and Jiang, L. Z., "A Boundary Integral Formulation and 2D Fundamental Solution for Piezoelectric Media," *Mechanical Research Communications*, Vol. 21, No. 1, 1994, pp. 47–54.

[28] Lee, J. S., "Boundary Element Method for Electroelastic Interaction in Piezoceramics," *Engineering Analysis with Boundary Elements*, Vol. 15, No. 4, 1995, pp. 321–328.

[29] Denda, M., and Lua, J., "Development of the Boundary Element Method for 2D Piezoelectricity," *Composites: Part B*, Vol. 30, No. 7, 1999, pp. 699–707.

[30] Pan, E., "A BEM Analysis of Fracture Mechanics in 2D Anisotropic Piezoelectric Solids," *Engineering Analysis with Boundary Elements*, Vol. 23, No. 1, 1999, pp. 67–76.

[31] Chen, T., and Lin, F. Z., "Boundary Integral Formulations for Three-Dimensional Anisotropic Piezoelectric Solids," *Computational Mechanics*, Vol. 15, No. 6, 1995, pp. 485–496.

[32] Hill, L. R., and Farris, T. N., "Three-Dimensional Piezoelectric Boundary Element Method," *AIAA Journal*, Vol. 36, No. 1, 1998, pp. 102–108.

[33] Davì, G., "General Theory for Cross-Ply Laminated Beam," *AIAA Journal*, Vol. 35, No. 8, 1997, pp. 1334–1340.

[34] Davì, G., and Milazzo, A., "Boundary Element Solution for the Free Edge Stresses in Composite Laminates," *Journal of Applied Mechanics,* Vol. 64, No. 4, 1997, pp. 877–884.

[35] Davì, G., and Milazzo, A., "Boundary Integral Formulation for Composite Laminates in Torsion," *AIAA Journal*, Vol. 35, No. 10, 1997, pp. 1660–1666.

[36] Davì, G., and Milazzo, A., "Bending Stress Fields in General Composite Laminates," *Computers and Structures*, Vol. 71, No. 3, 1999, pp. 267–276.

[37] Milazzo, A., "Interlaminar Stresses in Composite Laminates Under Out-of-Plane Shear/Bending," *AIAA Journal*, Vol. 38, No. 4, 2000, pp. 687–694.

[38] Davì, G., and Milazzo, A., "Piezoelectric Composite Laminates," *Proceedings of the International Conference on Computational Engineering and Sciences (ICES)*, Vol. 1, Tech Science Press, Forsyth, GA, 2000, pp. 87–92.

[39] Davì, G., and Milazzo, A., "Electroelastic Analysis of General Piezoelectric Composite Laminates by Boundary Integral Equations," *Proceedings of the First MIT Conference on Computational Fluid and Solid Mechanics*, Vol. 2, Elsevier, Amsterdam, 2001, pp. 1116–1119.

[40] Davì, G., and Milazzo, A., "Stress and Electric Fields in Piezoelectric Composite Laminates," *Proceedings of the 2nd International Conference on Boundary Element Techniques*, Hoggar, Geneva, 2001, pp. 137–144.

[41] Barnett, D. M., and Lothe, J., "Dislocations and Line Charges in Anisotropic Piezoelectric Insulators," *Physical Review B: Solid State*, Vol. 67, No. 1, 1975, pp. 105–111.

[42] Lekhnitskii, S. G., *Theory of Elasticity of an Anisotropic Body*, Holden-Day, San Francisco, 1963.

[43] Chue, C. H., and Chen, C. D., "Decoupled Formulation of Piezoelectric Elasticity Under Generalized Plane Deformation and Its Application to Wedge Problems," *International Journal of Solids and Structures*, Vol. 39, No. 12, 2002, pp. 3131–3158.

[44] Tiersten, H. F., *Linear Piezoelectric Plate Vibration*, Plenum, New York, 1969.

[45] Davì, G., and Milazzo, A., "Multidomain Boundary Integral Formulation for Piezoelectric Materials Fracture Mechanics," *International Journal of Solids and Structures*, Vol. 38, No. 40–41, 2001, pp. 7065–7078.

[46] Banerjee, P. K., and Butterfield, R., *Boundary Element Methods in Engineering Science*, McGraw–Hill, New York, 1981.

[47] Davì, G., "A General Boundary Integral Formulation for the Numerical Solution of Bending Multilayer Sandwich Plates," *Proceedings of the 11th International Conference on Boundary Element Methods*, Vol. 1, Computational Mechanics, Southampton, England, U.K., 1989, pp. 25–35.

[48] Tashiro, K., Tadokoro, H., and Kobayashi, M., "Structure and Piezoelectricity of Poly(Vinilidene Fluoride)," *Ferroelectrics*, Vol. 32, No. 2, 1981, pp. 167–175.

[49] Whitcomb, J. D., Raju, I. S., and Goree, J. G., "Reliability of the Finite Element Method for Calculating Free Edge Stresses in Composite Laminates," *Computers and Structures*, Vol. 15, No. 1, 1982, pp. 23–37.

[50] Wang, S. S., and Choi, I., "Boundary-Layer Effects in Composite Laminates: Part 1—Free Edge Stress Singularities," *Journal of Applied Mechanics*, Vol. 49, No. 3, 1982, pp. 541–548.

[51] Wang, S. S., and Choi, I., "Boundary-Layer Effects in Composite Laminates: Part 2—Free Edge Stress Solutions and Basic Characteristics," *Journal of Applied Mechanics*, Vol. 49, No. 3, 1982, pp. 549–560.

[52] Davì, G., and Milazzo, A., "Boundary-Layer Effects in Piezoelectric Composite Wedges," *Proceedings of the XVII National Congress of Associazione Italiana di Aeronautica e Astronautica*, Vol. 1, Associazione Italiana di Aeronautica e Astronautica, Rome, 2003, pp. 529–538.

S. Saigal
Associate Editor